Remote Sensing of Environment xxx (xxxx) xxx–xxx

Contents lists available at ScienceDirect

Remote Sensing of Environment

journal homepage: www.elsevier.com/locate/rse

Nocturnal Light Emitting Diode Induced Fluorescence (LEDIF): A new technique to measure the chlorophyll *a* fluorescence emission spectral distribution of plant canopies in situ

Jon Atherton[a,*], Weiwei Liu[b], Albert Porcar-Castell[a]

[a] Optics of Photosynthesis Laboratory, Institute for Atmospheric and Earth System Research/Forest Sciences, University of Helsinki, Finland
[b] LREIS, Institute of Geographic Sciences and Natural Resources Research, Chinese Academy of Sciences, 100101, China

ARTICLE INFO

Keywords:
LEDIF
Chlorophyll a fluorescence
Plant functional traits
FAST2017

ABSTRACT

- Solar induced chlorophyll *a* Fluorescence (SIF), which is distributed over a relatively broad (~200 nm) spectral range, is a signal intricately connected to the efficiency of photosynthesis and is now observable from space. Variants of the Fraunhofer Line Depth/Discriminator (FLD) method are used as the basis of retrieval algorithms for estimating SIF from space. Although typically unobserved directly, recent advances in FLD-based algorithms now facilitate the prediction (by model inversion) of the canopy emitted fluorescence spectrum from the discrete-feature FLD retrievals.
- Here we present first canopy scale measurements of chlorophyll *a* fluorescence spectra emitted from Scots pine at two times of year, and also from a lingonberry dominated understory. We used a high power multispectral Light Emitting Diode (LED) array to illuminate the respective canopies at night and measured under standardised conditions using a field spectrometer mounted in the nadir position above the canopy. We refer to the technique, which facilitates the in situ upscaling of a commonly measured leaf scale quantity to the canopy, as nocturnal LED-Induced chlorophyll *a* Fluorescence (LEDIF).
- The shape of the LEDIF spectra was dependant on the colour of the excitation light and also on the dominant species. Because we measured pine at two different times of year we were also able to show an increase in the canopy scale apparent quantum yield of fluorescence which was consistent with leaf-level increase in fluorescence yield recorded with a monitoring PAM fluorometer.
- The automation of the LEDIF technique could be used to estimate seasonal changes in canopy fluorescence spectra and yield from fixed or mobile platforms and provide a window into functional traits across species and architectures. LEDIF could also be used to evaluate FLD and inversion-based retrievals of canopy spectra, as well as different irradiance normalisation schemes typically applied to SIF data to account for the dependence of SIF on ambient light conditions.

1. Introduction

Vegetation acts as the main terrestrial sink of carbon dioxide in the planetary carbon cycle via the process of photosynthesis. Therefore measuring and forecasting the response of vegetation to changes in climate is a key aim of global change research, and such efforts require estimates of Gross Primary Production (GPP) at the landscape scale (Forkel et al., 2016). At the ecosystem scale, the eddy covariance technique is used to measure surface carbon exchange and derive estimates of GPP locally, but to accurately scale across continents remote sensing data are required. Broadband vegetation indices (VIs) such as the Normalized Difference Vegetation Index (NDVI) or Enhanced Vegetation Index (EVI), have traditionally filled this role and found wide-scale application in the remote sensing of terrestrial GPP from space (Beer et al., 2010; Forkel et al., 2016). However over the past decade an alternate method, which is potentially more responsive to short time scale changes in photosynthetic activity than VIs, has gained traction; the remote sensing of solar-induced fluorescence (SIF) (Porcar-Castell et al., 2014; Frankenberg and Berry, 2017).

SIF is a passive remote sensing measure of chlorophyll *a*

* Corresponding author.
E-mail address: jon.atherton@helsinki.fi (J. Atherton).

https://doi.org/10.1016/j.rse.2019.03.030
Received 2 November 2018; Received in revised form 18 February 2019; Accepted 22 March 2019

fluorescence, and therefore originates in vivo from within the photosynthetic organs of plants which occur primarily in leaves. Hence SIF depends on the leaf area of a canopy, and also responds near-instantaneously to changes in the partitioning of the light dependant reactions of photosynthesis (Porcar-Castell et al., 2014). The responsiveness of SIF to changes in the photosynthetic reactions is the potential advantage of SIF in comparison to VIs, the majority of which are typically assumed to be uncoupled from short time scale intra-daily changes in photosynthetic dynamics. This is especially true for evergreen vegetation where chlorophyll content and by extension leaf level light absorption, remains relatively stable during the winter to summer photosynthetic transition period whereas fluorescence has been shown to increase markedly (Ensminger et al., 2004, Porcar-Castell et al., 2008a, Porcar-Castell et al., 2012, Bowling et al., 2018). At the regional scale, there is also evidence that SIF has the potential to track boreal forest temporal photosynthetic dynamics with increased accuracy when compared to VIs (Walther et al., 2016; Jeong et al., 2017).

SIF is retrieved from airborne, satellite and tower platforms using some variant of the Fraunhofer Line Depth/Discriminator (FLD) algorithm, which estimates SIF in narrow, dark regions of the electromagnetic spectrum caused by molecular light absorption (Meroni et al., 2009; Guanter et al., 2013; Frankenberg and Berry, 2017). In early airborne work, Plascyk (1975) developed instrumentation to estimate SIF from within heliospheric Fraunhofer lines, which is also the approach used by current satellite remote sensing algorithms (Frankenberg and Berry, 2017). The FLD method can also be applied to the Earth's atmospheric absorption features such as the telluric regions found around 760 nm and 687 nm known as the O_2A and O_2B features respectively after the element responsible for absorption (Meroni et al., 2009; Guanter et al., 2013). Although now used routinely to retrieve terrestrial fluorescence from space, perhaps the main limitation of the SIF method is that although SIF is distributed across a relatively broad spectral range (~650–850 nm), fluorescence as measured by the FLD is observable only at the discreet intervals where light absorption occurs.

Recent advances in spectral fitting methods address the above limitation by reconstructing the full emission spectrum by combining FLD measurements at multiple absorption features (Zhao et al., 2014, 2018; Cogliati et al., 2015). Such a reconstruction is desirable as it facilitates the scaling up of spectral parameters currently observable at the leaf scale to the canopy, such as the red far-red fluorescence peak ratio, which can be used to estimate leaf chlorophyll content (Hák et al., 1990; Buschmann, 2007). Further, the difference between canopy and leaf emission spectra provides insight into radiative transfer processes that occur at these scale intersections (Liu et al., 2017; Yang and Van Der Tol, 2018). Spectral reconstruction methods solve an inverse problem and rely on prior assumptions of the shape of the emission distribution to constrain the solution; this information is ultimately derived from simulations. In Zhao et al. (2014, 2018) and Cogliati et al. (2015) these simulations were generated by the Soil Canopy Observation Photochemistry and Energy (SCOPE) model (Van der Tol et al., 2009). Therefore although it is possible to predict and reconstruct canopy leaving fluorescence spectra, such predictions are un-validated due to the lack of any direct measurements of canopy scale spectra.

Chlorophyll *a* fluorescence spectra are relatively easy to measure at the leaf scale in the laboratory (Hák et al., 1990; Magney et al., 2017; Rajewicz et al., In review) and also in the field (Van Wittenberghe et al., 2013). Usually a low pass filter is employed to facilitate excitation but remove the contribution of reflected light from the measured signal. Once measured, SIF spectra can be statistically related to plant functional traits such as Specific Leaf Area or pigment contents (Van Wittenberghe et al., 2015; Atherton et al., 2017). However, as it is the canopy that is the typical target object in remote sensing, it is therefore the canopy emission spectrum that is of primary relevance. Of the little empirical work examining spectral fluorescence at the canopy scale, Zarco-Tejada et al. (2003) measured the superimposition of fluorescence spectra on canopy reflectance spectra for a small canopy and revealed a double-peak shape. More recently, Carstensen et al. (2016) developed a greenhouse-based system measuring fluorescence emitted from basil plant canopies using a multi-colour LED illumination system. Also recently, Romero et al. (2018) measured fluorescence spectra emitted by a small fig tree placed within a darkened wooden box. In this work Romero et al. (2018) developed a physically based set of equations to quantify the effect of light re-absorption at the leaf and whole tree scale, and therefore relate the canopy leaving fluorescence spectrum to the spectrum emitted from the chloroplasts within the leaf. This was motivated by the fact that light re-absorption is an important control on the shape of the fluorescence spectrum, particularly in the red region where the emission overlaps with the long tail of the chlorophyll absorption spectrum (Buschmann, 2007).

As far as we are aware there have been no previous attempts to measure chlorophyll *a* fluorescence spectra emitted from whole plant canopies in the field. In light of this, our aim was to develop and test a new methodology to measure chlorophyll *a* fluorescence spectral emission distributions in situ. Here we show how fluorescence emission spectra are observable in the field at night, with the aid of a powerful multi-spectral Light Emitting Diode (LED) light source; we refer to the technique as nocturnal LED-Induced chlorophyll *a* Fluorescence, or LEDIF. During 2017, we measured both Scots pine over-story at two different times of year, and lingonberry dominated under-story canopy to demonstrate the technique and explore the influence of temporal photosynthetic dynamics unrelated to changes in incident sunlight, and also species on the canopy leaving fluorescence spectrum.

2. Methods

2.1. Measurement site

Canopy spectral measurements of Scots pine (*Pinus sylvestris* L.) over-story and the predominantly lingonberry (*Vaccinium vitis-idaea* L.) under-story were carried out during May and September 2017, as a part of the Fluorescence Across Space and Time (FAST2017) campaign, at the Station for Measuring Atmosphere-Ecosystem Relations II (SMEARII), Hyytiälä, Finland (61°51N, 24°17E). Site measurements of above canopy photosynthetically active radiation (PAR) and in canopy (16.8 m) temperature were downloaded from the publicly accessible SMARTSMEAR database (https://avaa.tdata.fi/web/smart).

2.2. Canopy spectral measurements

Canopy scale steady state chlorophyll *a* fluorescence spectra were excited at night using a multispectral LED light source (BPP210 Beamz Professional, distributed by Tronios BV, Twente, Netherlands) from a scaffold tower at a height of approximately 0.5 m above a mature 15 m tall Scots pine tree (Fig. 1). Our initial measurements from pine were in the early hours of 00:00–01:30 17th May 2017, which we repeated later in the season at 21:30–23:30 6th September 2017. Measurements during summer were not practical due to absence of dark nights during boreal summer.

The light source consists of an array of 18 separate 4-in-1 multi-colour LEDs which are rated at 12 W each, where the 4-in-1 refers to the human colour perception of light sources settings; Red-Green-Blue-White. The light source was positioned in slightly off-nadir position to increase the illuminated proportion of the tree (Fig. 2 shows a similar pine tree illuminated by the same light source, albeit at a greater above canopy distance). An ASD handheld spectroradiometer (Malvern Panalytical, Boulder, USA), with FWHM 3.5 nm; spectral sampling interval of 1.6 nm; spectral range of 325–1075 nm, was attached to the tower in the nadir position, approximately 1.1 m above the light source, or 1.6 m above the top of the tree canopy. This was operated in bare fiber mode, characterised by a field of view angle of 25° and at a vertical distance of 1.6 m, resulting in spot radii at the top of canopy and base of the tree as (approximately) 0.35 m and 3.7 m respectively.

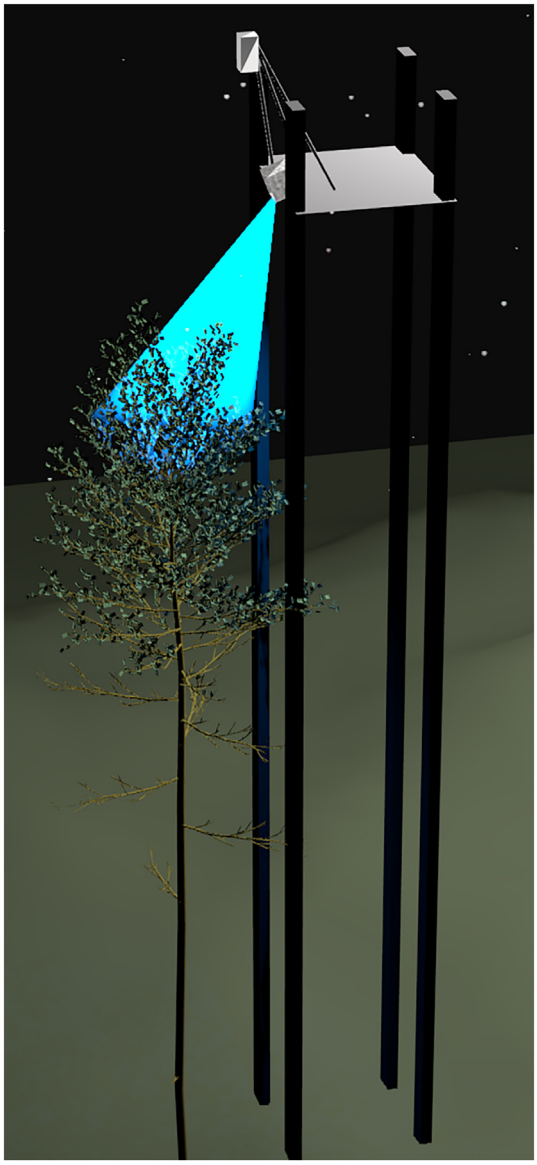

Fig. 1. Illustrative measurement set-up for Scots pine. Spectrometer and LED light source are mounted in nadir and off-nadir positions respectively above top of canopy. Measurements are carried out at night, which enables the measurement of canopy scale spectra in situ without the reflected contribution of the target contaminating the measurement. Note that in the measurements presented in this study, the tree canopy was not a single isolated crown but belonged to a semi-closed continuous cover forest.

In addition to the pine measurements, on the 5th of September between 21:30 and 23:30 we carried out measurements of the vegetative under-story, which predominantly consisted of lingonberry. For the lingonberry the light-source was mounted 140 cm above the canopy, and the spectrometer was in nadir view attached to tripod 90 cm above the canopy. In our May LEDIF measurements we tested a range of (long) integration times: 278,528 ms (~4 1/2 min.), 557,056 ms (~9 min) and 139,264 ms (~2 1/3 min). All of these times resulted in reasonably accurate spectra (no smoothing required), so in the September measurements we used the shorter of the three integration times (139,264 ms) to conduct all measurements. Blue, green and red LED settings were used to excite fluorescence and were measured one after the other; the spectral distributions of the light source are shown in Fig. 2. Dark current corrections were collected prior to measurements, after switching the lamp colour. The long integration time of the dark current and subsequent spectral fluorescence measurements, together with the relatively low quantum doses (< 25 μmol/m^2/sr/nm), helped to ensure that spectra were collected in the steady-state mode (limited Kautsky/fluorescence decay dynamics). Due to the longer integration times and lower air temperatures in the May measurements, we collected two repeats for each excitation colour (with the exception of green where the repeat failed). Because we used shorter integration times during the September measurements, we were able to collect more repeats (between 3 and 13 depending on the sample). Except for the green-excited May pine measurement (n = 1), we calculated the mean spectrum for each repeat; we also calculated the standard deviations for the repeats.

Hemispherical directional reflectance factors of the two canopies were approximated by taking daytime measurements of the ratio of incident irradiance reflected by the two canopies to subsequent measurements of sky irradiance reflected by an (approximately) Lambertian white PTFE panel (Decagon Devices, Washington, USA) using the ASD spectrometer described above.

2.3. Spectral fluorescence reflectance contribution correction and apparent quantum yield estimation

We developed a simple correction for the spectral overlap of the red excitation and emission distributions. This was necessary because if left uncorrected reflected light in the spectral overlap region distorts the fluorescence emission spectrum: specifically, for the red illumination setting where there is significant overlap between excitation (E) and emission (F) wavelengths (Fig. 2). Hence, the correction removes the reflected contribution from the emitted spectrum by assuming the measured (uncorrected) spectrum (F_u) is a combination of reflected and fluoresced radiance:

$$F(\lambda) = F_u(\lambda) - r(\lambda)\frac{E(\lambda)}{\pi} \quad (1)$$

where F is the corrected spectrum, and r is the canopy reflectance. E was estimated by scaling a laboratory measured spectral distribution of LED irradiance to estimated incident irradiance reflected by the canopy (see Appendix A.1 for description of incident irradiance estimation). The reason we measured this in the laboratory was because we had difficulty mounting the white panel at the precise top of canopy location of incident irradiance, however there is no reason why E could not be estimated directly in the field given suitable infrastructure. The laboratory measurement set-up consisted of an Ocean Optics USB2000 spectrometer and 400 μm fiber optic cable (both Ocean Optics Inc., Florida, U.S.A.) connected to the top (vertical axis) port of 6 in. diameter integrating sphere (Labsphere Inc., North Sutton, N.H., U.S.A.). The experimental LED light source was pointed to one of the sphere ports covered with a circular diffuser sheet (80°, Luminit LSD®, CA, U.S.A.). Measurements were collected at an integration time of 50 ms, and spectral averaging was set to 100.

Normalising spectral fluorescence by incident radiation is required to allow the comparison of (steady state) spectra obtained under different lighting conditions, and is analogous to the estimation of reflectance factors in field spectroscopy. The apparent quantum yield (AQY) of a canopy is the number of fluoresced photons escaping the canopy divided by the number of photons absorbed by a canopy, and can be estimated from measurements of spectral fluorescence converted to quantum (mol of photons) units (F_q, μmol/m^2/s/sr/nm):

$$AQY = \frac{number\ of\ photons\ emitted}{number\ of\ photons\ absorbed} = \frac{\pi \int F_q\ d\lambda}{APAR} \quad (2)$$

where $APAR$ is Absorbed Photosynthetically Active Radiation ($APAR$). In this study, $APAR$ was estimated as a function of the canopy reflectance factor and incident irradiance (see Appendix A.1 for a spectral definition of $APAR$). (Note that when we applied 2 we integrated over a reduced spectral emission range of 670–800 nm to avoid distortion artefacts due in part to overcorrection of the red excited spectra, see

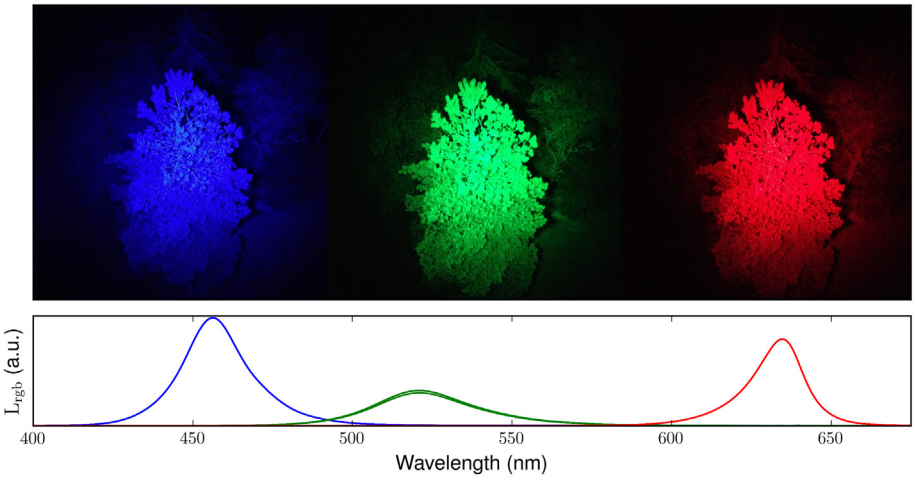

Fig. 2. Example of Scots pine illuminated during night by the LED source for each of the colour settings. Each illumination colour shown above (blue, green, red) was used to excite chlorophyll fluorescence, and resulted in different shaped chlorophyll fluorescence emission spectra when measured with an above canopy spectrometer. The spectral distributions of the three light colours pictured above are shown in the lower panel. (For interpretation of the references to colour in this figure legend, the reader is referred to the web version of this article.)

Fig. 3). Omitting the integral from the numerator in 2 results in the yield distribution (yield per emission nm) which was calculated using mean spectra:

$$AQY(\lambda) = \frac{\pi}{APAR} F_q(\lambda) \quad (3)$$

Note that since the LED light source provides only a small amount of actinic light to the foliage we do not expect it to trigger any significant regulatory response in terms of non-photochemical quenching, although it could potentially generate some photochemical quenching response thereby increasing the signal relative to the minimal F_0 state as typically measured by Pulse Amplitude Modulated (*PAM*) fluorometer systems. Both the spectrally resolved LEDIF and the PAM measured fluorescence emission depend on the intensity and properties of the measuring light, the sample PAR absorption, the structure and properties of the sample, as well as the quantum yield of fluorescence. Accordingly, *AQY* could be thought as a canopy-level homology of the

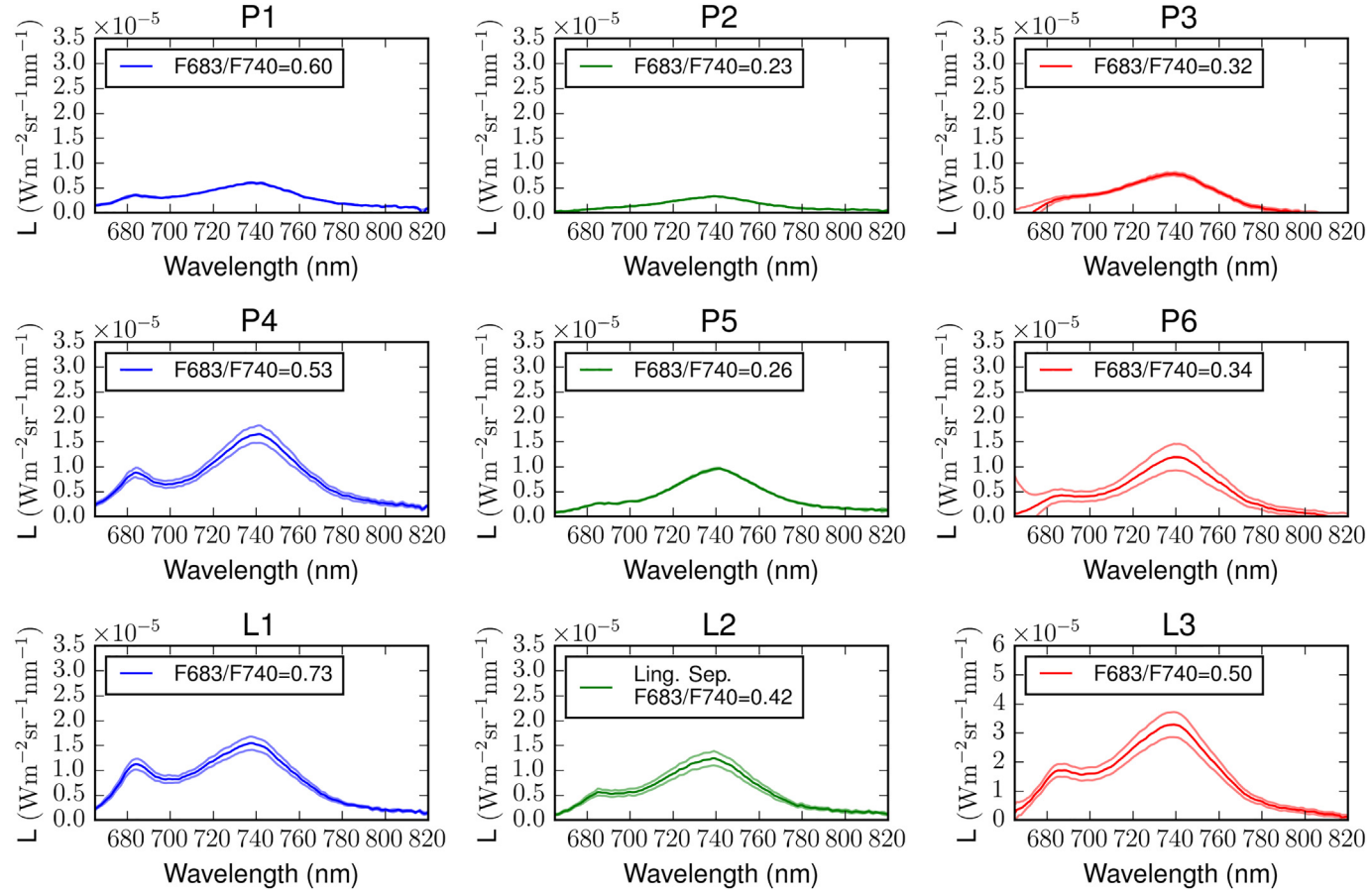

Fig. 3. Canopy scale chlorophyll fluorescence emission spectral distributions. Top row are Scots pine measured in May, middle row are Scots pine measured in September and bottom row are predominantly lingonberry under-story measured in September. Spectra are coloured according to the colour of the excitation (illumination) spectrum, which also corresponds to column order (from left to right; blue, green, red). Note the different Y-axis scale for red excited lingonberry. Solid lines are mean spectra, and faded lines are mean spectra ± 1 SD. (For interpretation of the references to colour in this figure legend, the reader is referred to the web version of this article.)

photosystem level quantum yield of fluorescence (Porcar-Castell et al., 2014), with the difference that the former is also affected by the re-absorption within the leaf and canopy.

2.4. Supporting data

In addition to nocturnal canopy LEDIF measurements, we also measured the operating quantum yield of photochemistry of pine needles with a Monitoring PAM fluorometer system (Porcar-Castell et al., 2008b; Porcar-Castell, 2011). The Monitoring PAM is an active fluorometer system (Maxwell and Johnson, 2000) capable of measuring PAR, Temperature, steady state (F') and maximal fluorescence yield (F_m') at multiple locations and repeatedly over time. In this study, three independent fluorometers were deployed across the top canopy of three different pine trees, which included a probe located in the top canopy of the same tree used for LEDIF measurements. Data was used to derive the operating quantum yield of photosystem II $[(F_m' - F')/F_m']$ as well as the quantum yield of fluorescence and constitutive thermal energy dissipation ($\Phi_{F,D}$) a leaf level proxy of the quantum yield of fluorescence (see Porcar-Castell, 2011 for details, but note the unfortunate typo in Eq. (24) therein, where F_M' should be F_{MR}, the summer reference maximal fluorescence yield). Midnight levels (± 30 min) of Φ_{PSII} (corresponding to the widely used F_v/F_m) and $\Phi_{F,D}$ were subsequently used to discuss the leaf level dynamics between May and September and compared to the apparent quantum yields derived from LEDIF.

3. Results

3.1. Fluorescence and illumination spectral distributions

The relative spectral distributions of the illumination source are presented in Fig. 2, which shows how the long tail of the red illumination distribution slightly overlaps with the chlorophyll *a* fluorescence emission region in the red wavelengths. Fig. 2 also shows digital photography of the reflected radiance of the light source from an example tree.

Spectral fluorescence data collected during May and September 2017 are shown in Fig. 3. The spectral overlap of the excitation source with emission wavelengths is clear for all red-excited spectra, resulting in obviously distorted spectra (panels p3, p6, L3 in Fig. A.3). For pine measured in September, and also understory spectra, the spectral overlap correction was (qualitatively) successful, significantly changing the shape of the spectrum (solid lines in right most graphs in Fig. 3) and reducing the fluorescence in the near-red region to expected values based on a priori knowledge of leaf emission spectra (Atherton et al., 2017). For pine spectra measured in May with red LED light the correction was less successful, resulting in physically implausible negative values at wavelength extrema. Likely over-correction also occurred in the other red LEDIF spectra given the simple correction method that we used, which is visible in the May pine spectrum due to the relatively low signal measured at this time.

For both species, the familiar double peak shape is well defined in blue-excited emission spectra, but less so in green or red-excited spectra. For lingonberry blue-excited *F683/F740* was substantially higher than for either of the pine measurements (0.73 Vs 0.53/0.6). In absolute terms red spectra were typically greater in magnitude than blue and green excited spectra, however such a result is limited in information due to the dependence of the spectrum on the amount of incident PAR, motivating the calculation of *AQY* values reported below.

AQY Spectra (fluorescence in quantum units and normalized by *APAR*) are shown in Fig. 4. For pine, there was a clear increase in *AQY* from May to September, especially for green and red excitation wavelengths. Additionally, the *AQY* of lingonberry was larger, by a factor of at least two, compared to the pine measured over the same time period. The *AQY* with red excitation light was consistently higher across dates and for both plant canopies. In lingonberry, spectral fluorescence was much greater across wavelengths for red excited spectra than other excitation colours and pine (Fig. 3, lower right panel). In contrast, lingonberry *AQY* values for red excited light were relatively similar to the other excitation colours (Fig. 4, bottom row).

3.2. Supporting measurements

PAR during all observational periods was 0 μmol/m^2/s, which was a necessary condition for successful measurements. Temperatures immediately prior to the earlier observational period (16th May) had a larger diurnal range than in September. Although midnight temperatures were similar in both May (5.73 °C at 00:00), and September (5.57 °C and 7.52 °C at 00:00 on the 6th and 7th September, respectively). *PAR* incident above the canopy as well temperature during the observational periods is shown in Fig. A.4, where the observational periods are marked on the figure as vertical grey bars.

When comparing fluorescence yields estimated from spectral data (as *AQY*) to MONI-PAM observations, the percentage of increase in quantum yield calculated for the blue excitation light using fluorescence spectra from May to September was 92%, 102% for the green light and 56% for the corrected red light. For the MONI-PAM the corresponding increase in $\Phi_{F,D}$ was 77%, and increase in F_v/F_m was 39%.

4. Discussion

4.1. LEDIF: a new method to measure canopy scale spectra

In this study we presented what are, to our knowledge, the first reported in situ field measurements of nocturnal Light Emitting Diode induced chlorophyll *a* fluorescence spectra (LEDIF) emitted from mature plant canopies (Fig. 3). This was achieved by exciting chlorophyll molecules at night time using a powerful multi-spectral light source. Using this technique we measured fluorescence spectral distributions emitted by two contrasting canopy architectures within the same ecosystem; Scots pine over-story, which was measured at two different times of year, and lingonberry dominated under-story.

Under natural illumination conditions a much larger proportion of radiation incident on a canopy is scattered (reflected) than is fluoresced by chlorophyll molecules. As a consequence, and although chlorophyll *a* fluorescence is emitted across a relatively broad spectrum in the red to near infra-red wavelengths, the canopy scale chlorophyll *a* fluorescence spectrum remains effectively hidden from observation and solar-induced fluorescence from space is retrieved only at specific wavelength intervals within the spectrum using the FLD method (Plascyk, 1975; Frankenberg and Berry, 2017). Hence at both the ecosystem (tower) and satellite pixel scale, the spectral component of the signal remains obfuscated. Considering this, we developed the LEDIF method to measure the previously unobserved canopy leaving fluorescence spectra in situ. The shape of the canopy spectrum is of interest in theoretical research because it is determined by both the physiology (photosynthesis) of the canopy, but also the 3 dimensional structure of the canopy (Liu et al., 2017) which can introduce vegetation specific deviation in SIF-GPP relationships when observed at the ecosystem and satellite pixel scales (Migliavacca et al., 2017; Sun et al., 2017; Zhang et al., 2018).

Although not measured under natural illumination directly, there have been previous attempts to estimate the canopy leaving fluorescence spectral distribution using (simulated) FLD observations, which fall under the umbrella of spectral reconstruction techniques (Cogliati et al., 2015; Zhao et al., 2014). Both the spectral fitting method developed by Cogliati et al. (2015) and the Singular Value Decomposition method by Zhao et al. (2014) used model simulations of multiple-feature FLD retrievals to estimate the canopy leaving spectrum. When (qualitatively) comparing the reconstructed spectra in these two studies to the spectra measured here, we find that our observed spectra show a tendency to lower red to far red ratios than the reconstructed spectra in

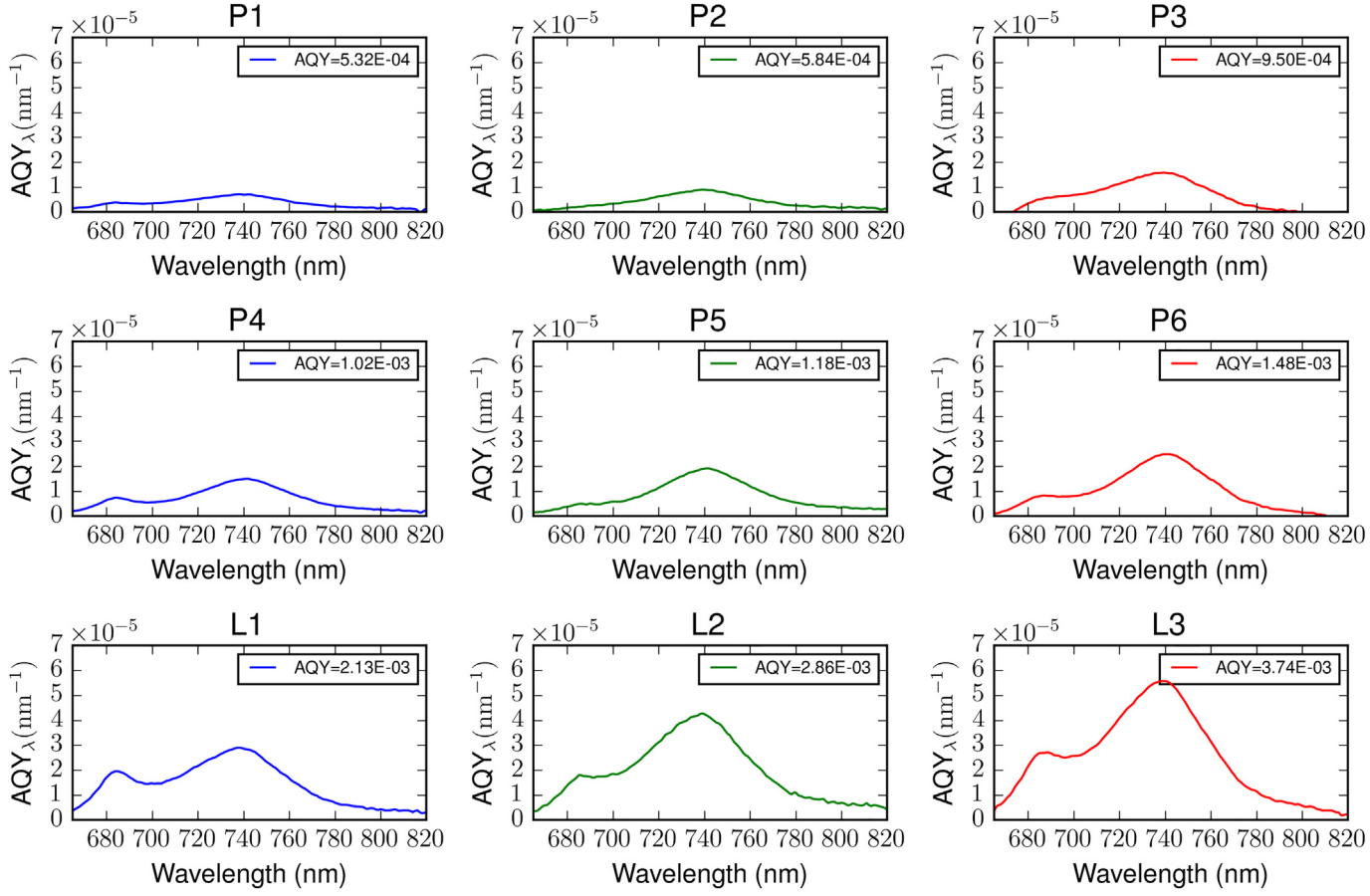

Fig. 4. Spectral distributions of fluorescence canopy apparent quantum yield. Top row are Scots pine measured in May, middle row are Scots pine measured in September and bottom row are predominantly lingonberry under-story measured in September. Spectra are coloured according to the colour of the excitation (illumination) spectrum, which also corresponds to column order (from left to right; blue, green, red). Integrated yield values are shown in the legends.

these studies (Fig. 3). However, it is difficult to make any firm conclusions from such a comparison. Firstly, the canopy leaving spectrum is known to depend on the excitation spectrum, which was not the same across these studies. Secondly these studies relied extensively on simulated data, generated by the SCOPE (Van der Tol et al., 2009) model, and in the case of Zhao et al. (2014) supplemented with measurements of a crop species (maize). Potentially, the LEDIF method presented here could be applied to the validation of such schemes.

In addition to spectral reconstruction techniques, there have also been limited attempts at spectral measurements of canopy leaving fluorescence. In an early study by Zarco-Tejada et al. (2003) reflectance difference spectra were used to estimate the change in shape due to fluorescence dynamics. However, because these measurements were reflectance difference measurements, rather than directly measured spectra they cannot be directly compared to those in our study as they reflect the fluorescence spectral properties of the variable fluorescence component typically associated to photosystem II only (Porcar-Castell et al., 2014), rather than the total fluorescence. In addition to the difference spectra presented in Zarco-Tejada et al. (2003), very recently Romero et al. (2018) measured spectra emitted by a *Ficus* plant excited with a blue LED. As with our Scots pine measurements these spectra were heavily weighted towards the far red, with resultantly small *F683/F740* values. However, it should also be pointed out that in the present study, and in contrast to Romero et al. (2018), we used a multi-spectral light source to illuminate mature canopies in-situ and demonstrated a strong dependency of the resulting emission shape on the excitation spectrum at the larger scale.

This phenomenon, which is well known at the leaf scale (Buschmann, 2007; Atherton et al., 2016; Magney et al., 2017), occurs because different colours (wavelengths) of light have different penetration depths into the absorbing/fluorescing material, and resultantly differing emission, re-absorption and scattering profiles. In more detail; blue photons are preferentially absorbed closer to the top of the canopy whereas red and especially green photons penetrate to greater depths (Vogelmann and Evans, 2002). Therefore, those fluorescence photons excited by blue light typically have a shorter path to travel out of the canopy than those excited by other colours, this lowers the probability of subsequent canopy interactions (re-absorption and scattering) for these photons. This discrepancy presents itself as differences in red far red ratios as a function of excitation colour, qualitatively the double peak shape is more pronounced in blue excited spectra. Here we measured this result at the canopy scale (Fig. 3).

At the photosystem scale, within leaves, chlorophyll *a* fluorescence is distributed as a relatively broad emission spectrum with a high maximum in the red (~680 nm), and a second peak at a much smaller magnitude in the near-infrared (~740 nm), commonly referred to as the far red peak (Pedrós et al., 2008). On existence from the leaf, this spectral shape is completely transformed with the red peak being reduced to a similar magnitude to the far-red peak; it is at this scale the familiar double-peak signature of the fluorescence spectrum occurs, with typical red to far red peak (*F683/F740*) ratios clustered below unity for steady state spectra (Van Wittenberghe et al., 2013, 2015; Atherton et al., 2017; Rajewicz et al., In review). When up-scaling again the from the leaf to canopy, re-absorption is further enhanced, and the red peak is reduced in magnitude again (relative to the far-red peak), as is evident in our canopy scale spectra. Additionally, when we compared our canopy scale measurements to leaf level data measured in a laboratory for the same species (Rajewicz et al., In review), we found that

leaf level *F683/F740* values were generally similar (~0.5) to canopy value (Fig. 3), noting that the light sources and times of year were not consistent across these two studies.

In contrast to the red-emission wavelengths, far red fluorescence is less affected by chlorophyll re-absorption. The escape probability of far red fluorescence depends more on the structure of the canopy which controls scattering (Huang et al., 2007; Stenberg et al., 2013; Yang and Van Der Tol, 2018). Given the above, it is not surprising that we observed differences in spectral shape between pine and lingonberry dominated sub-canopies, where the higher red far-red ratios observed in lingonberry for blue excited light point to the reduced effect of re-absorption in comparison to pine. There were also large differences in fluorescence yield for the two species (Fig. 4), which were likely due to some combination of differences in whole plant and leaf architecture. We speculate that this is because lingonberry's broad leaves are arranged in a carpet-like structure on the forest floor whereas Scots pine has needle like leaves which are rather sparsely arranged through a much deeper canopy which affects both the magnitude and shape of the measured spectra.

In the absence of simultaneously acquired leaf and canopy spectra (measured at precisely the same time) it not possible to conclude which processes (re-absorption, scattering) occurs at which scale and for which species. However such simultaneous measurements are feasible and could also be used to provide empirical evidence for the theoretical link between canopy reflectance and far red SIF recently proposed by Yang and Van Der Tol (2018), where the scattering of far red SIF is parameterised as a function of reflectance, leaf albedo and canopy interception parameters.

In addition to the scattering and re-absorption related processes described above, the canopy leaving emission spectrum is also affected by the dynamics of the photosynthetic light reactions. This is because the quantum yield of chlorophyll fluorescence is directly controlled by photochemical and non-photochemical energy conversion processes in the photosystems (Porcar-Castell et al., 2014). In the present study we observed a clear increase in apparent spectral yields for all colours, from May to September for pine, which was consistent with the observed increase in the maximum quantum yield of photochemistry (F_v/F_m) and chlorophyll fluorescence and basal thermal energy dissipation ($\Phi_{F,D}$), as measured with a Monitoring PAM system in the same pine canopy (Fig. 4 and Table 1). The increase in F_v/F_m and $\Phi_{F,D}$ from May to September reflects the seasonal dynamics in the acclimation of the light reactions of photosynthesis, where measurements in May were conducted with the canopy still experiencing substantial levels of photosynthetic downregulation (F_v/F_m = 0.469, Table 1). Measurements in September were conducted towards the end of the growing season under much smaller downregulation levels (F_v/F_m = 0.653).

Winter downregulation is related to the accumulation of sustained forms of non-photochemical quenching, NPQ (Verhoeven, 2014), and has been shown to quench the leaf-level fluorescence signal in Scots pine (Porcar-Castell, 2011; Porcar-Castell et al., 2012), which we expected to influence the canopy level spectral measurements. The increase in MONIPAM fluorescence yield between May and September evenings registered at 77%, driven by the seasonal reduction of sustained NPQ. The comparable increase in *AQY* in the blue excited spectrum, as the MONIPAM uses a blue light to excite fluorescence, was higher at 92%. Although in approximate agreement, the discrepancies between the relative MONIPAM and LEDIF yield increases are likely due to uncertainties relating to both the spectral observations and the derived *AQY* estimates which we discuss in detail below.

Table 1
Chlorophyll fluorescence parameters derived from MONIPAM and canopy spectral data for Scots pine. MONIPAM parameter were the combined yield of fluorescence and basal thermal energy dissipation ($\Phi_{F,D}$) and maximum photochemical yield (F_v/F_m). AQY values were derived from spectral data.

Date	$\Phi_{F,D}$	$\Delta\Phi_{F,D}$ [relative to 17.5.2017]	F_v/F_m	$\Delta F_v/F_m$ [relative to 17.5.2017]	*AQY* [b/g/r]	ΔAQY [relative to 17.5.2017, b/g/r]
17.5.2017	0.130	–	0.469	–	5.32E−4, 5.84E−4, 9.50E−4	–
7.9.2017[a]	0.230	77%	0.653	39%	1.02E−3, 1.18E−3, 1.48E−3	92%, 102%, 56%

[a] Note that AQY values in September were acquired late evening on 6th September, hence 'Date' refers to date of closest midnight (00:00).

4.2. Uncertainties and methodological limitations

As a small number of repeat measurements from the same target were collected within a relatively short time window, within spectrum variation (error) was probably unrelated to differences in vegetation structure. It is also unlikely that there were significant physiological differences causing these deviations in time during individual measurement periods, which leaves the possibility of instrumental error, caused by temperature fluctuations for example, as a likely cause of variation in fluorescence radiance spectra. The small number of repeats across samples (Fig. A.4) was partially a consequence of the long integration times used for the measurements. Addressing this issue by increasing the light source irradiance or via the automated sampling of spectra over longer time periods would permit more accurate uncertainty estimates from repeat measurements. A lower spectral resolution instrument could also be used to increase the signal to noise ratio and decrease the integration time, which is a necessary requirement for measurements from mobile platforms.

Uncertainties in the estimated *AQY* values relate to each of the quantities used in the estimation, namely spectral fluorescence, canopy reflectance and incident irradiance. In addition, the larger errors in the red-excited spectra for radiance spectra relative to other colours are a consequence of the fact that these spectra were corrected using reflectance measurements, whose errors were propagated. The correction to the red spectrum resulted in negative values at longer wavelengths, particularly in the pine data collected in May. Nonetheless, the effect of spectral overlap clearly has a large influence on uncorrected red-excited spectra (Fig. A.4), necessitating the correction.

We used the same pine canopy reflectance spectrum, which was measured in September, to calculate *AQY* values and correct red spectra for both May and September data-sets. In actuality, the growth of new pine shoots between these dates likely caused a small change in pine reflectance, however if propagated through Eq. (2) this would result in only a minor difference in yields relative to the observed increases. The assumption of constant reflectance between May and September would introduce a small error in *APAR* due to the mis-estimation of *fAPAR*. Further errors in the *APAR* estimation could also be due to the absorption of light by non-green canopy elements and also due the spatial variation of the incident light source.

Additionally, although we tried to position the spectrometer in the same position above the canopy in May and September the field of view might not have been identical on these two occasions. Hence it is possible that September observations measured a slightly different fraction of the crown relative to May observations. Differences in the proportion of canopy gap relative to filled crown, due again to positional field of view mismatch, could also be a possible explanation for the increase in radiance observed between May and September. We reason that our derived *AQY* values were largely insensitive to mismatches in position between May and September as we estimated incident irradiance as a function of radiance reflected during the fluorescence measurement itself, resulting in *AQY* values that were independent of the fluorescent source area measured.

In our irradiance estimation technique, we fitted laboratory measured light source spectra to saturated, and hence distorted, field

measured spectra of reflected radiance (see Appendix A.1). Hence, incorrect estimations of incident irradiance could have arisen due to spectral distortion of the field measured spectra and caused resultant errors in derived *AQY* values. A practical step to reduce uncertainty in irradiance estimation would be to use a (mechanised) Lambertian white panel or calibrated irradiance sensor in the canopy to measure irradiance immediately prior or post measurements.

Finally, it should also be noted that the LEDIF measurements are a function of both incident light direction, and also observer direction. Although we measured both species in the nadir direction, the light source direction was slightly off-nadir, which could have potentially biased the comparison of LEDIF spectra from different species. Directional LEDIF anisotropy could be quantified using a field goniometer such as the system recently developed by Biriukova et al. (2018) for SIF measurements.

With these caveats in mind, we suggest that future measurements should be under taken from a fixed mounting point in continuous nightly operation to further test the hypotheses that nocturnal LEDIF spectra can be used to study seasonal dynamics in canopy scale photosynthetic activity. Despite the caveats and uncertainties discussed above, the spectral yield calculations standardised our spectra to fixed (repeatable) lighting conditions, and allowed spectra collected under differing conditions to be compared.

5. Conclusions and future development of nocturnal LEDIF

We demonstrated that canopy scale spectral measurements of chlorophyll *a* fluorescence spectra are not only possible, but also potentially informative of plant functional dynamics and architectural traits. In our study we used a multi-spectral light emitting diode source to induce fluorescence for a pine overstory and a lingonberry dominated understory canopy. In the present study we demonstrated the viability of the technique in a field setting, however there are several ways in which the LEDIF technique could be developed and improved which we outline below:

1. *Development of light source*. We used a commercially available light source manufactured for the entertainment industry which was limited in terms of power, and which resultantly restricted the illumination field to a single pine tree canopy. To increase the number of trees under illumination and consider a true 'canopy' of multiple crowns, a light source of several kW would likely be required. Increasing the power of the light source (or individual LEDs) would also increase the signal to noise ratio which would result in shorter integration times, which is a necessary requirement for canopy scale measurements from mobile platform (e.g. drones). In addition, the temperature stability of the light source should also be considered for making the measurements repeatable and output illumination monitored during measurements for correction during post-processing.
2. *Reflectance contribution correction*. We used a simple reflectance-based method to correct the contribution of the red radiation to the emission spectrum. However, this method resulted in over-correction especially for the May measurements (Fig. 3, P3). The use of appropriate filters in combination with the light source would be a practical step to restrict the 'cross-over' of the source and emission regions, although this may be a costly option for an array of LEDs. In addition, in this study we did not consider the effects of spectral stray light (Zong et al., 2006). Such effects relate to the limited resolution of the spectrometer itself, characterised by the spectrometer line spread function, and have been shown to slightly distort leaf fluorescence emission spectra (Rajewicz et al., In review). A more comprehensive correction could also tackle this issue.
3. *Solar-induced spectrum reconstruction and use in FLD algorithms*. The spectral distributions (and yields) presented here were measured relative to different excitation spectra at night time. Hence the (daytime) solar induced spectrum remains unmeasured. Given appropriate constraints (relating to smoothness and correlation) the measured spectra could be used to solve the inverse problem of estimating the full Excitation Emission Matrix from a limited number of measurements, which is required to predict the solar induced spectrum. This opens the method up for direct use in validating current FLD-based retrieval algorithms.

In summary there are two main applications of our new method; firstly to validate fluorescence spectral distributions either partially (via spectral fitting methods) or wholly predicted by models, and secondly to monitor seasonal changes in chlorophyll *a* fluorescence spectra of whole plant canopies.

Acknowledgements

Jon Atherton and Albert Porcar-Castell were funded by the Academy of Finland (project numbers 288039, 293443 and 319211). Weiwei Liu has been co-financed by the University of Chinese Academy of Sciences (UCAS [2015] 37) Joint PhD Training Program and the Academy of Finland (project numbers 293443 and 288039).

Appendix A

A.1. Estimation of irradiance and APAR from spectral measurements

We required top of canopy APAR estimates to derive apparent quantum fluorescence yield (AQY) values (Section 2.3). In the field, spectral irradiance (*E*) is typically estimated by measuring the radiance reflected by a white near-Lambertian panel in the downward looking (nadir) position. In this study it was not practical to measure the panel at night above the canopy, hence we used a simple empirical method to estimate the irradiance incident at the top of the canopy. This was achieved by combining estimates of canopy reflectance factor, reflected radiance measured during the night-time, and laboratory measurements of the spectral distribution of the light sources (L_{rgb}) in the following protocol:

1. Canopy reflectance factors (r) were first estimated during the daytime by dividing the radiance reflected by the pine tree or lingonberry canopy by that from a near Lambertian panel using the same handheld ASD spectrometer used for spectral fluorescence measurements. The canopy reflectance spectra are shown in Fig. A.2.
2. As the reflected radiance (in the excitation/illumination region) from the tree (L_{toc}) was also measured during the night time as a by-product of the spectral fluorescence measurements, if the canopy reflectance spectrum is also known, then the spectral irradiance incident at the top of the canopy (E_{toc}) can be estimated as:

$$E_{toc}(\lambda) = \frac{\pi\, L_{toc}(\lambda)}{r(\lambda)} \tag{a.1}$$

3. However because of the need to optimise the integration time for spectral fluorescence measurements, pixel values in the reflected radiance

portion of the spectrum were saturated at most (but not all) wavelengths. This issue was overcome by fitting the laboratory measured spectral light distributions to a single unsaturated radiance value from the night-time fluorescence measurements. This resulted in 3 wavelength independent scale factors [$a_{rgb} = L_{toc}(\lambda = unsat.) / L_{rgb}(\lambda = unsat.)$], which were used to substitute the (mainly) saturated reflected radiance spectra with the laboratory spectra to estimate irradiance incident at the top of the caopy (E_{toc})

$$E_{toc}(\lambda) \approx \frac{\pi\ a_{rgb}\ L_{rgb}(\lambda)}{r(\lambda)} \tag{a.2}$$

4. Next we converted E_{toc} to units of quanta (E_q, μmol/m^2/s/nm) to estimate incident spectral photosynthetically active radiation using the Planck-Einstein relation and Advogadro's constant.
5. Finally, spectral Absorbed Photosynthetically Active Radiation (APAR) was estimated from the canopy reflectance factor (r) and spectral PAR (E_q) as:

$$APAR = fAPAR\ PAR = \int_{400\ nm}^{700\ nm} A\ E_q\ d\lambda \approx \int_{400\ nm}^{700\ nm} (1 - r)\ E_q\ d\lambda \tag{a.3}$$

where A is the fraction of absorbed PAR (fAPAR) at each measured wavelength interval. Note that using $1 - r$ to approximate A disregards the effects of canopy transmittance and soil reflectance, which will result in a small error in the calculation.

A.2. Canopy reflectance spectra

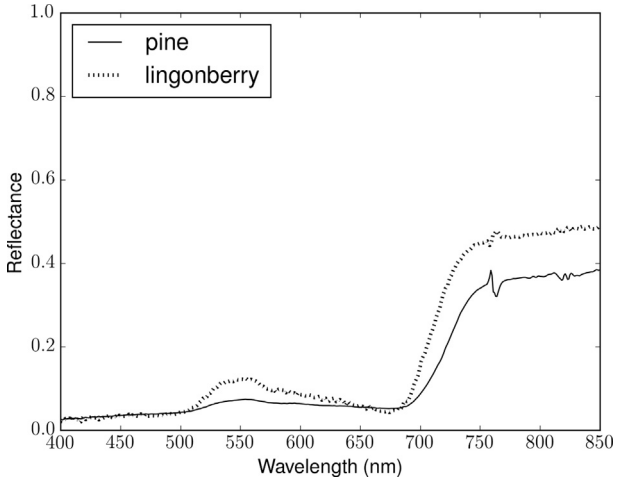

Fig. A.2. Canopy reflectance spectra for pine canopy and lingonberry canopies in September 2017.

A.3. Spectral fluorescence data

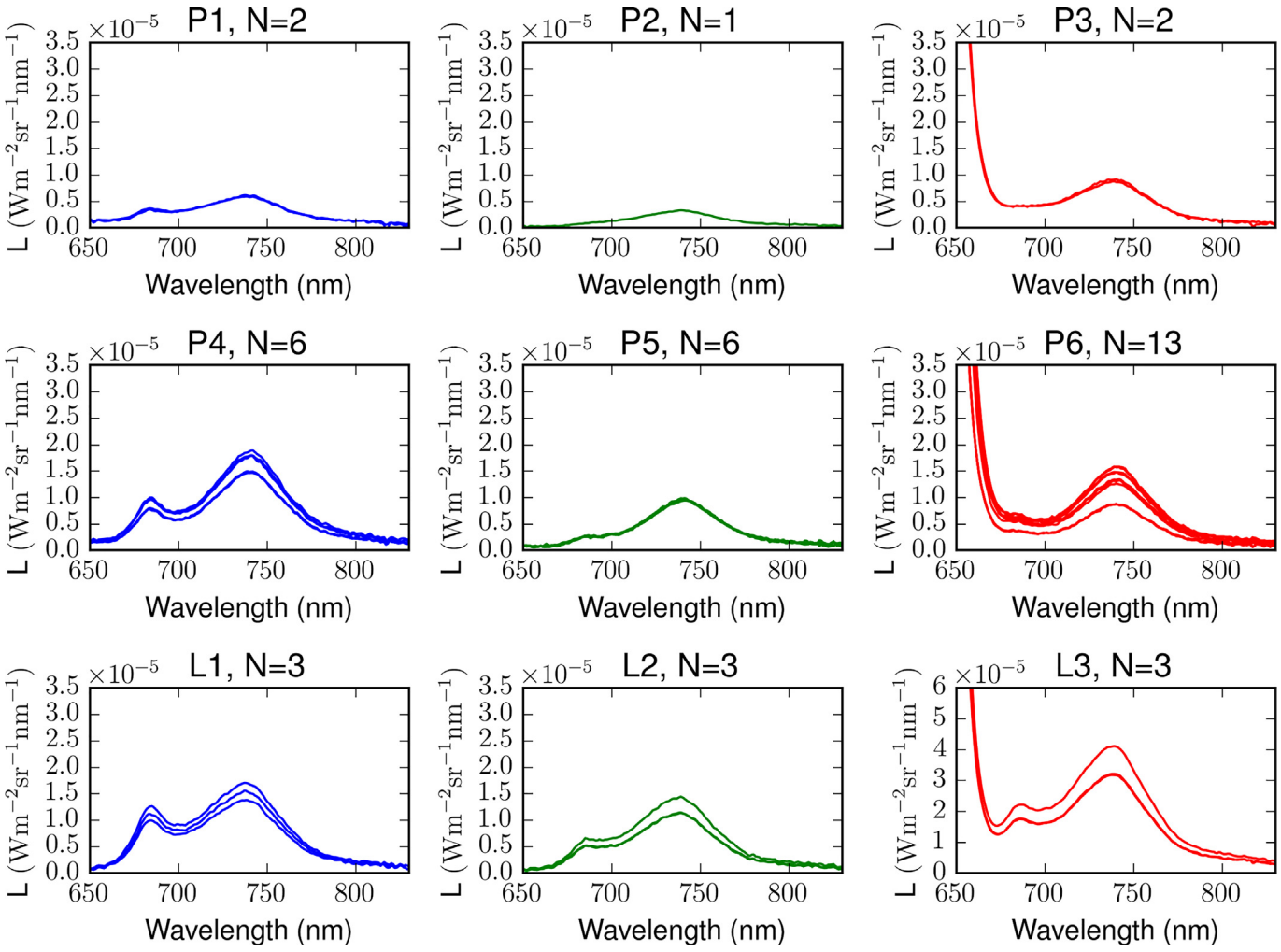

Fig. A.3. All measurements of canopy scale chlorophyll fluorescence emission spectral distributions. Top row are Scots pine measured in May, middle row are Scots pine measured in September and bottom row are predominantly lingonberry under-story measured in September. Spectra are coloured according to the colour of the excitation (illumination) spectrum. For red excited spectra, uncorrected spectra are as solid lines. Note the different Y-axis scale for red excited lingonberry.

A.4. Environmental variables timeseries

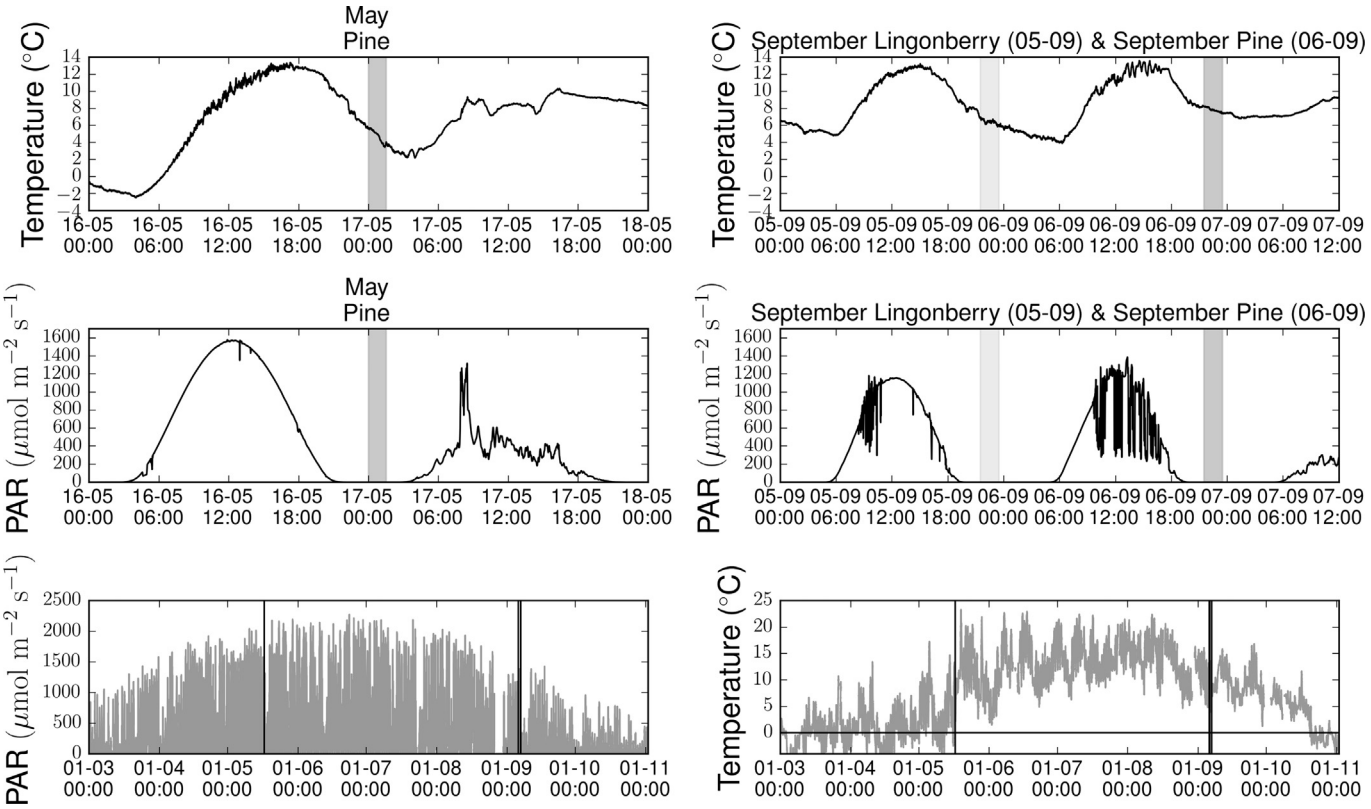

Fig. A.4. Environmental conditions during the measurement periods. The grey vertical bars mark the time of canopy spectral fluorescence measurements. Photosynthetic dynamics typically lag temperature by a number of days. Hence the May measurements occurred prior to the full spring recovery of photosynthesis (see lower right panel).

References

Atherton, J., Nichol, C.J., Porcar-Castell, A., 2016. Using spectral chlorophyll fluorescence and the photochemical reflectance index to predict physiological dynamics. Remote Sens. Environ. 176, 17–30.

Atherton, J., Olascoaga, B., Alonso, L., Porcar-Castell, A., 2017. Spatial variation of leaf optical properties in a boreal forest is influenced by species and light environment. Front. Plant Sci. 8.

Beer, C., Reichstein, M., Tomelleri, E., Ciais, P., Jung, M., Carvalhais, N., Rödenbeck, C., Arain, M.A., Baldocchi, D., Bonan, G.B., Bondeau, A., 2010. Terrestrial gross carbon dioxide uptake: global distribution and covariation with climate. Science 329 (5993), 834–838.

Biriukova, K., Julitta, T., Celesti, M., Panigada, C., Evdokimov, A., Migliavacca, M., Rossini, M., 2018. Characterisation of reflectance and chlorophyll fluorescence anisotropy defining requirements for an experimental setup. In: EGU General Assembly Conference Abstracts. 20. pp. 16936.

Bowling, D.R., Logan, B.A., Hufkens, K., Aubrecht, D.M., Richardson, A.D., Burns, S.P., Anderegg, W.R., Blanken, P.D., Eiriksson, D.P., 2018. Limitations to winter and spring photosynthesis of a Rocky Mountain subalpine forest. Agric. For. Meteorol. 252, 241–255.

Buschmann, C., 2007. Variability and application of the chlorophyll fluorescence emission ratio red/far-red of leaves. Photosynth. Res. 92 (2), 261–271.

Carstensen, A.M., Pocock, T., Bånkestad, D., Wik, T., 2016. Remote detection of light tolerance in Basil through frequency and transient analysis of light induced fluorescence. Comput. Electron. Agric. 127, 289–301.

Cogliati, S., Verhoef, W., Kraft, S., Sabater, N., Alonso, L., Vicent, J., Moreno, J., Drusch, M., Colombo, R., 2015. Retrieval of sun-induced fluorescence using advanced spectral fitting methods. Remote Sens. Environ. 169, 344–357.

Ensminger, I., Sveshnikov, D., Campbell, D.A., Funk, C., Jansson, S., Lloyd, J., Shibistova, O., Öquist, G., 2004. Intermittent low temperatures constrain spring recovery of photosynthesis in boreal Scots pine forests. Glob. Chang. Biol. 10 (6), 995–1008.

Forkel, M., Carvalhais, N., Rödenbeck, C., Keeling, R., Heimann, M., Thonicke, K., Zaehle, S., Reichstein, M., 2016. Enhanced seasonal CO2 exchange caused by amplified plant productivity in northern ecosystems. Science 351 (6274), 696–699.

Frankenberg, C., Berry, J., 2017. Solar induced chlorophyll fluorescence: origins, relation to photosynthesis and retrieval. In: Reference Module in Earth Systems and Environmental Sciences, https://doi.org/10.1016/B978-0-12-409548-9.10632-3.

Guanter, L., Rossini, M., Colombo, R., Meroni, M., Frankenberg, C., Lee, J.E., Joiner, J., 2013. Using field spectroscopy to assess the potential of statistical approaches for the retrieval of sun-induced chlorophyll fluorescence from ground and space. Remote Sens. Environ. 133, 52–61.

Hák, R., Lichtenthaler, H.K., Rinderle, U., 1990. Decrease of the chlorophyll fluorescence ratio F690/F730 during greening and development of leaves. Radiat. Environ. Biophys. 29 (4), 329–336.

Huang, D., Knyazikhin, Y., Dickinson, R.E., Rautiainen, M., Stenberg, P., Disney, M., Lewis, P., Cescatti, A., Tian, Y., Verhoef, W., Martonchik, J.V., 2007. Canopy spectral invariants for remote sensing and model applications. Remote Sens. Environ. 106 (1), 106–122.

Jeong, S.J., Schimel, D., Frankenberg, C., Drewry, D.T., Fisher, J.B., Verma, M., Berry, J.A., Lee, J.E., Joiner, J., 2017. Application of satellite solar-induced chlorophyll fluorescence to understanding large-scale variations in vegetation phenology and function over northern high latitude forests. Remote Sens. Environ. 190, 178–187.

Liu, W., Atherton, J.M., Mottus, M., MacArthur, A., Teemu, H., Maseyk, K., Robinson, I., Honkavaara, E., Porcar Castell, J.A., 2017. Upscaling of solar induced chlorophyll fluorescence from leaf to canopy using the dart model and a realistic 3D forest scene. In: The International Archives of the Photogrammetry, Remote Sensing and Spatial Information Sciences.

Magney, T.S., Frankenberg, C., Fisher, J.B., Sun, Y., North, G.B., Davis, T.S., Kornfeld, A., Siebke, K., 2017. Connecting active to passive fluorescence with photosynthesis: a method for evaluating remote sensing measurements of Chl fluorescence. New Phytol. 215 (4), 1594–1608.

Maxwell, K., Johnson, G.N., 2000. Chlorophyll fluorescence—a practical guide. J. Exp. Bot. 51 (345), 659–668.

Meroni, M., Rossini, M., Guanter, L., Alonso, L., Rascher, U., Colombo, R., Moreno, J., 2009. Remote sensing of solar-induced chlorophyll fluorescence: review of methods and applications. Remote Sens. Environ. 113 (10), 2037–2051.

Migliavacca, M., Perez-Priego, O., Rossini, M., El-Madany, T.S., Moreno, G., van der Tol, C., Rascher, U., Berninger, A., Bessenbacher, V., Burkart, A., Carrara, A., 2017. Plant functional traits and canopy structure control the relationship between photosynthetic CO2 uptake and far-red sun-induced fluorescence in a Mediterranean grassland under different nutrient availability. New Phytol. 214 (3), 1078–1091.

Pedrós, R., Moya, I., Goulas, Y., Jacquemoud, S., 2008. Chlorophyll fluorescence emission spectrum inside a leaf. Photochem. Photobiol. Sci. 7 (4), 498–502.

Plascyk, J.A., 1975. The MK II Fraunhofer line discriminator (FLD-II) for airborne and orbital remote sensing of solar-stimulated luminescence. Opt. Eng. 14 (4), 144339.

Porcar-Castell, A., 2011. A high-resolution portrait of the annual dynamics of photochemical and non-photochemical quenching in needles of Pinus sylvestris. Physiol. Plant. 143 (2), 139–153.

Porcar-Castell, A., Juurola, E., Ensminger, I., Berninger, F., Hari, P., Nikinmaa, E., 2008a. Seasonal acclimation of photosystem II in Pinus sylvestris. II. Using the rate constants of sustained thermal energy dissipation and photochemistry to study the effect of the light environment. Tree Physiol. 28 (10), 1483–1491.

Porcar-Castell, A., Pfündel, E., Korhonen, J.F., Juurola, E., 2008b. A new monitoring PAM fluorometer (MONI-PAM) to study the short-and long-term acclimation of photosystem II in field conditions. Photosynth. Res. 96 (2), 173–179.

Porcar-Castell, A., Garcia-Plazaola, J.I., Nichol, C.J., Kolari, P., Olascoaga, B., Kuusinen, N., Fernández-Marín, B., Pulkkinen, M., Juurola, E., Nikinmaa, E., 2012. Physiology of the seasonal relationship between the photochemical reflectance index and photosynthetic light use efficiency. Oecologia 170 (2), 313–323.

Porcar-Castell, A., Tyystjärvi, E., Atherton, J., van der Tol, C., Flexas, J., Pfündel, E.E., Moreno, J., Frankenberg, C., Berry, J.A., 2014. Linking chlorophyll a fluorescence to photosynthesis for remote sensing applications: mechanisms and challenges. J. Exp. Bot. 65 (15), 4065–4095.

Rajewicz, P.A., Atherton, J., Alonso, L., Porcar-Castell, A., 2019. Leaf-level spectral fluorescence measurements: comparing methodologies for broadleaves and needles. Remote. Sens. 11 (5), 532.

Romero, J.M., Cordon, G.B., Lagorio, M.G., 2018. Modeling re-absorption of fluorescence from the leaf to the canopy level. Remote Sens. Environ. 204, 138–146.

Stenberg, P., Lukeš, P., Rautiainen, M., Manninen, T., 2013. A new approach for simulating forest albedo based on spectral invariants. Remote Sens. Environ. 137, 12–16.

Sun, Y., Frankenberg, C., Wood, J.D., Schimel, D.S., Jung, M., Guanter, L., Drewry, D.T., Verma, M., Porcar-Castell, A., Griffis, T.J., Gu, L., 2017. OCO-2 advances photosynthesis observation from space via solar-induced chlorophyll fluorescence. Science 358 (6360), eaam5747.

Van der Tol, C., Verhoef, W., Timmermans, J., Verhoef, A., Su, Z., 2009. An integrated model of soil-canopy spectral radiances, photosynthesis, fluorescence, temperature and energy balance. Biogeosciences 6 (12), 3109–3129.

Van Wittenberghe, S., Alonso, L., Verrelst, J., Hermans, I., Delegido, J., Veroustraete, F., Valcke, R., Moreno, J., Samson, R., 2013. Upward and downward solar-induced chlorophyll fluorescence yield indices of four tree species as indicators of traffic pollution in Valencia. Environ. Pollut. 173, 29–37.

Van Wittenberghe, S., Alonso, L., Verrelst, J., Moreno, J., Samson, R., 2015. Bidirectional sun-induced chlorophyll fluorescence emission is influenced by leaf structure and light scattering properties—a bottom-up approach. Remote Sens. Environ. 158, 169–179.

Verhoeven, A., 2014. Sustained energy dissipation in winter evergreens. New Phytol. 201 (1), 57–65.

Vogelmann, T.C., Evans, J.R., 2002. Profiles of light absorption and chlorophyll within spinach leaves from chlorophyll fluorescence. Plant Cell Environ. 25 (10), 1313–1323.

Walther, S., Voigt, M., Thum, T., Gonsamo, A., Zhang, Y., Köhler, P., Jung, M., Varlagin, A., Guanter, L., 2016. Satellite chlorophyll fluorescence measurements reveal large-scale decoupling of photosynthesis and greenness dynamics in boreal evergreen forests. Glob. Chang. Biol. 22 (9), 2979–2996.

Yang, P., Van Der Tol, C., 2018. Linking canopy scattering of far-red sun-induced chlorophyll fluorescence with reflectance. Remote Sens. Environ. 209, 456–467.

Zarco-Tejada, P.J., Pushnik, J.C., Dobrowski, S., Ustin, S.L., 2003. Steady-state chlorophyll a fluorescence detection from canopy derivative reflectance and double-peak red-edge effects. Remote Sens. Environ. 84 (2), 283–294.

Zhang, Z., Zhang, Y., Joiner, J., Migliavacca, M., 2018. Angle matters: bidirectional effects impact the slope of relationship between gross primary productivity and sun-induced chlorophyll fluorescence from Orbiting Carbon Observatory-2 across biomes. Glob. Chang. Biol. https://doi.org/10.1111/gcb.14427.

Zhao, F., Guo, Y., Verhoef, W., Gu, X., Liu, L., Yang, G., 2014. A method to reconstruct the solar-induced canopy fluorescence spectrum from hyperspectral measurements. Remote Sens. 6 (10), 10171–10192.

Zhao, F., Li, R., Verhoef, W., Cogliati, S., Liu, X., Huang, Y., Guo, Y., Huang, J., 2018. Reconstruction of the full spectrum of solar-induced chlorophyll fluorescence: Intercomparison study for a novel method. Remote Sens. Environ. 219, 233–246.

Zong, Y., Brown, S.W., Johnson, B.C., Lykke, K.R., Ohno, Y., 2006. Simple spectral stray light correction method for array spectroradiometers. Appl. Opt. 45 (6), 1111–1119.